An Electronic Tongue

An electronic tongue is a matrix of sensors that detect molecules (called *ligands* in this context) that cause the gustatory stimuli (i.e. the *flavors*). The construction and development of such sensors is actively studied due to their relevance and wide applicability in food analysis, pharmaceutical industry, biomedical research and security, among others. See e.g. Marx et al. [1] and Podrazka et al. [2] for numerous applications of the electronic tongue.

In this work, mostly based on the publication *Duplex Bioelectronic Tongue for Sensing Umami and Sweet Tastes Based on Human Taste Receptor Nanovesicles* (Ahn et al., 2016 [3]), I review some related literature, explain the operation of the electronic tongue constructed by Ahn et al. [3] and briefly cover the manufacturing stages, characterization processes and the tests results obtained.

Introduction

The sense of taste in mammals is determined by the presence and activity of sensory cells located in different parts of the oral epithelium, mainly in the epithelium of the tongue [4,5]. The fungiform, foliate and circumvalate papillae of the tongue gather these sensory cells, which is why they are called "taste buds" [4]. Each taste bud is made up of 50-100 sensory cells [4,5]. At the same time, five types of sensory cells can be differentiated (type I, II, III, IV and V cells) [4]. They are present in different proportions depending on the papilla [4,5], and directly responsible for the perception of taste [Figure 1] [5]. Sweet, umami and bitter tastes are detected by type II cells, and sour taste by type III cells [5]. Regarding the salty taste, in humans it is unknown which cell type is responsible for its reception [5,6], although research points to type II and III cells [4].
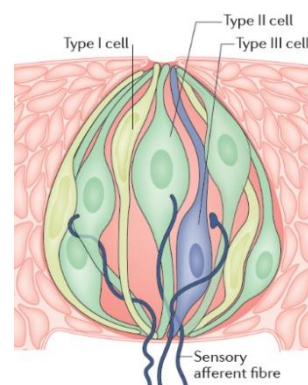

Figure 1.[5] Structure of a taste bud.

In the following, the biological mechanisms that allow us to detect and identify the different flavors are detailed, to later establish an analogy with the mechanism carried out in the electronic tongue.

- <u>Sweet, umami and bitter flavors</u>

Sweet, umami and bitter tastes are detected by type II cells [5] [Figure 2] [6], which have the following transmembrane receptor proteins: T1R2-T1R3 for detection of sweet ligands, T1R1-T1R3 for detection of umami ligands, and T2Rs for detection of bitter ligands [5]. When these cells are in a resting state, there is a difference in electrical potential between the inside and outside of the cell, known as the resting potential of the cell membrane [7,8]. This resting potential is due to the different ionic concentration between the inside and outside of the cell, and is a constant and stable potential to small disturbances [7]. When the ligand binds to its corresponding transmembrane receptor protein, a cascade of chemical signals is created which changes the ionic balance between both sides of the membrane, causing the transient depolarization of the cell membrane potential [7] (no longer resting). These transient voltage differences are known as action potentials [7], and in the type II cells they cause the opening of the voltage-gated channels CALHM1/CALHM3 [9], through which the neurotransmitter ATP is released. The released ATP is detected in the afferent nerve fibers by a receptor proteins that form ion channels that are activated (are opened and thus vary the ionic balance) when the ATP is received. A sufficient concentration of ATP is capable of generating action potentials in the nerve fibers, making the electrical signal reach the brain [4,6].
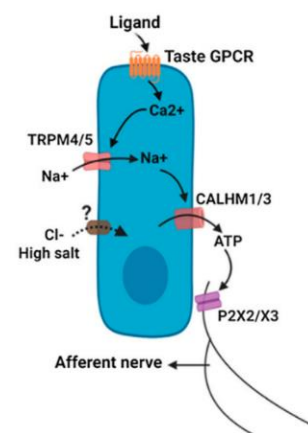

<u>Figure 2</u>.[6] Type II cell. The cascade of processes caused by the reception of a sweet, umami or bitter ligand is shown.

- <u>Sour taste</u>

Sour taste is detected by type III cells [5] [Figure 3] [6], which have protons selective channels OTOP1 (Otopetrin-1). The sour taste is associated with the entry of protons into the cell. When this happens, a cascade of chemical signals is created which changes the ionic balance between both sides of the membrane, causing the transient depolarization of the cell membrane potential [7]. These action potentials cause the release of the serotonin (5-HT), GABA and, possibly, norepinephrine neurotransmitters [10]. Results by Larson et al. [11] suggest that the released 5-HT is detected in the afferent nerve fibers by a receptor proteins that form ion

channels that are activated when the 5-HT is received [11]. A sufficient concentration of 5-HT will be capable of generating action potentials in the nerve fibers, making the electrical signal reach the brain. According to what I have been able to explore, the detection of GABA by the nerve fibers and the role of norepinephrine in the sense of taste haven't been resolved yet [5].

- ## Salty flavor

As mentioned before, in humans it is unknown which sensory cells are responsible for the reception and transduction of the signal [5,6].
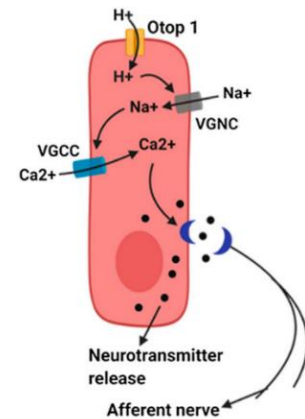
Figure 3.[6] Type III cell. The cascade of processes caused by the reception of a sour ligand is shown.

After this overview of the mechanisms carried out in the cells of the lingual epithelium for the reception of sweet, umami, bitter and sour flavors, the following explains how an electronic tongue works to emulate the sense of taste.

Electronic Tongue

An electronic tongue is an analytical instrument that comprises an array of sensors, which act selectively over different ligands [2,12]. The process by which each sensor in the matrix selectively detects a single ligand is called *selective sensing technique,* while the process by which each sensor in the matrix selectively detects a wide variety of ligands is called *cross-reactive array sensing technique* [12]. The *cross-reactive array sensing technique* is a bio-inspired approach that greatly increases the degree of heterogeneity of detectable ligands by sensors [12], bringing their capabilities closer to those developed by the biological sense of taste. Furthermore, this technique makes it possible to generate a "fingerprint" for each detected ligand. After treating the data, further unknown samples can be then recognized by comparing them to the learned fingerprints [12] [Figure 4] [12].
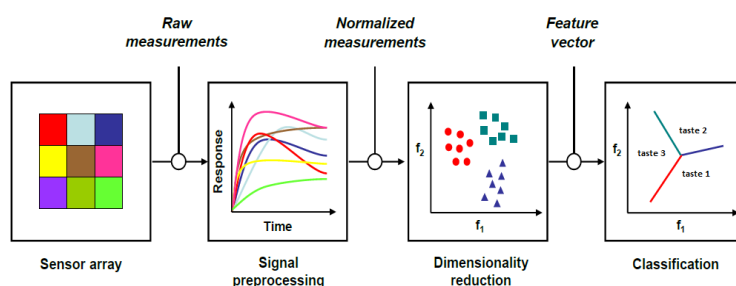
Figure 4. [12] Data processing and classification of the signals obtained by an array of cross-reactivity sensors.

In this work, an electronic tongue with an array of two cross-reactivity sensors is described: a sensor selectively detects various sweet ligands, and another sensor selectively detects various umami ligands. Furthermore, each sensor is made up of two fundamental components: a biomaterial that acts as a receptor for the ligand, and a (nano)material that acts as a transducer of the received signal (i.e. transforms a chemical signal into an electrical signal). The biomaterial is immobilized on the nanomaterial [13] [Figure 5] [13]. Here, the ligand receptor biomaterial is made up of nanovesicles built from human embryonic kidney 293 (HEK-293) cells, which express receptors for sweet and umami flavors in humans; and the material that acts as transducer of the received signal is graphene.
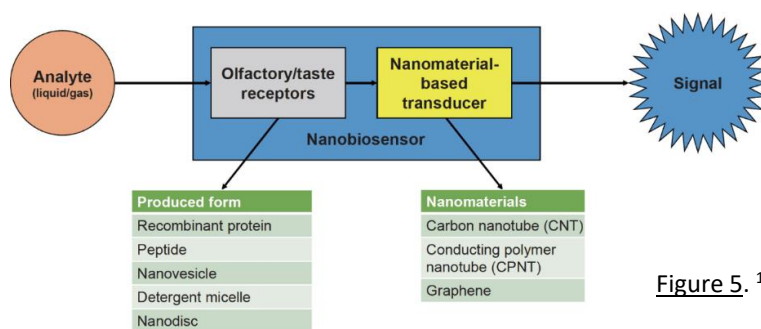

Figure 5. [13] Main components of a nanobiosensor.

• Functioning of the electronic tongue

The goal of the electronic tongue is to detect a chemical signal and transform it into an electrical signal. To make it, Ahn et al. [3] used graphene field-effect transistors (GFETs), on which they immobilized the nanovesicles.

A FET is a semiconductor electronic device with three terminals: Gate (G), Source (S), and Drain (D). Electric current flows between S and D, while G serves as modulator, since applying a voltage across G allows to control the conductivity between S and D, based on the electric field created. One quality that makes FET devices very promising instruments in the field of nanobiosensors is their amplification capacity, since with the application of very small voltages across G, very strong electrical signals can be achieved and modulated.

As for the graphene, it is a semiconductor material with a two-dimensional structure and exceptional electrical properties. The band gap of pristine graphene, that is, the energy required to promote an electron from the valence band to the conduction band, is zero [14]. This causes that pristine graphene to have a large ambipolar field effect when it is subjected to a gate voltage (a process called electrical doping) [14] [Figure 6] [14]. In this way it is possible to obtain a p-type semiconductor (the majority charge carriers are the holes) or an n-type

semiconductor (the majority charge carriers are the electrons) as a function of the applied gate voltage.

Ahn et al. [3] manufactured a GFET with two channels in order to detect sweet ligands through one of them, and umami ligands through the other one. The device consists of two pairs of S/D terminals (S_1/D_1 for one channel, and S_2/D_2 for the other channel), and a single multi-channel G terminal, through which gate voltages will be applied [Figure 7A] [3]. Constructed nanovesicles have receptor proteins (of sweet or umami ligand as appropriate) and ion channels in their membranes [Figure 7B] [3]. The sweet ligands receptor nanovesicles are immobilized on one of the graphene channels, between the D_x and S_x terminals, and the umami ligands receptor nanovesicles are immobilized on the other graphene channel, between the D_y and S_y terminals.
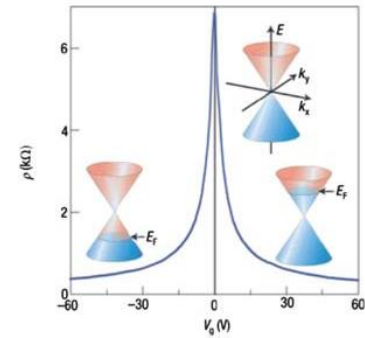
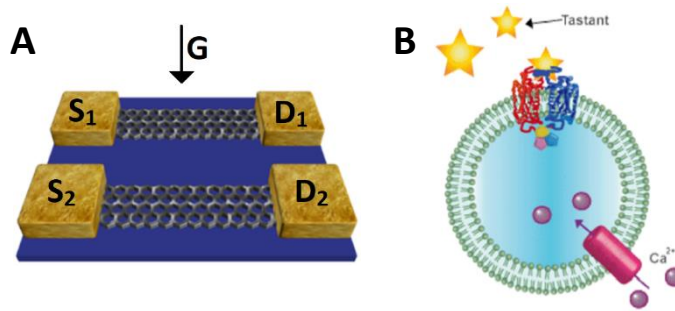Figure 6. [14] Ambipolar electric field effect on pristine graphene.

Figure 7. [3] (A) GFET designed by Ahn et al.; [3] (B) nanovesicles constructed by Ahn et al. [3].

Establishing an analogy with the processes described above for the reception of ligands by type II and III cells in humans, and the subsequent steps of them, and based on the experiments and observations of Ahn et al. [3], the operation of this electronic tongue can be described as follows: when the ligand (sweet or umami) binds to its corresponding transmembrane receptor protein in the nanovesicle, an intravesicular signaling process occurs that opens the ion channels, thus allowing the entry of Ca^{2+} cations into the vesicles*. This changes the ionic balance between both sides of the membrane, causing voltage differences. As previously mentioned, applying a voltage across G allows to control the conductivity between S and D, in based on the electric field created, so the electronic tongue allows establishing a relation between the concentration of ligand detected by the vesicles and the electrical signal measurement.

---

* "The signal change is due to the calcium influx from the outside of the cell or nanovesicle" (Ahn et al., 2016 [3]).

In order to test the electronic tongue, Ahn et al. [3] solubilized sweet flavorings and umami flavorings in DPBS (Dulbecco's Phosphate-Buffered Saline) saline solution which contained $CaCl_2$, as source of ions. This was done for different concentrations.

In the following, the manufacturing steps of a five-channel electronic tongue (representing the five basic flavors) are presented, according to the process carried out by Ahn et al. [3]. Subsequently, the characterizations and final results after testing the electronic tongue are shown (Ahn et al., 2016 [3]).

- <u>Manufacture of the electronic tongue</u> (stages carried out by Ahn et al. [3])

First, a monolayer of graphene grown by chemical vapor deposition [15] (CVD) is deposited, by dry transfer, on a silicon oxide substrate [Figure 7, step 1]. Next, by means of photolithography, the desired pattern is achieved on the graphene [Figure 7, stage 2]. Then, by means of a second photolithography, the positions of the contact electrodes (S and D) are defined [Figure 7, stage 3]. The electrodes are deposited by thermal evaporation of the Cr/Au metals [Figure 7, stage 4], followed by the lift-off process [16,17] [Figure 7, stage 5]. Finally, the device undergoes a passivation process [18] [Figure 7, stage 6].

Once the GFET device is built, and as explained above, it is time to immobilize the vesicles (biomaterial that acts as receptor for the ligand) on the graphene (material that acts as transducer of the received signal). For it, the graphene etchings are functionalized with pyrenebutyric acid *N*-hydroxysuccinimide ester (PSE) molecules, which act as linkers between the graphene and the vesicles [3].
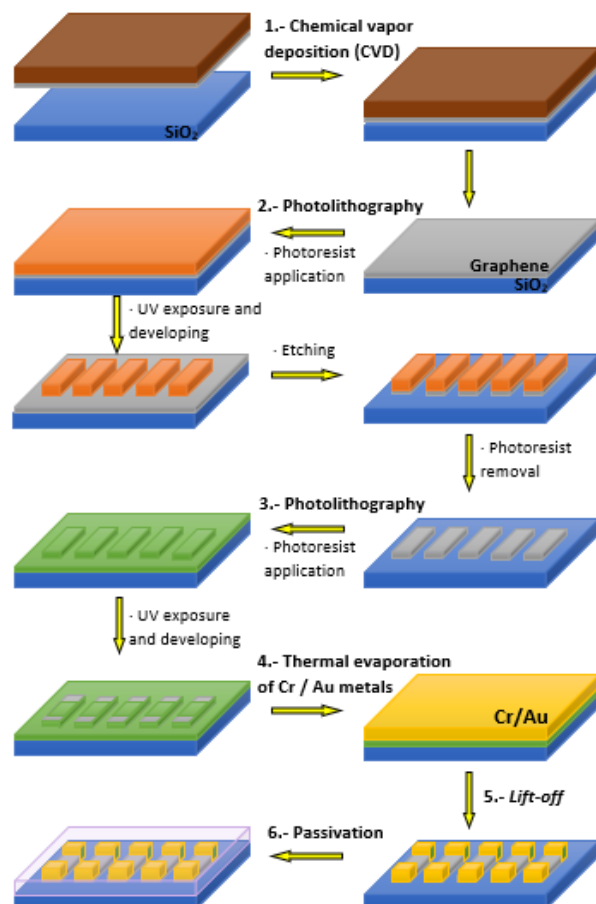
Figure 8. Manufacturing stages of the GFET device.

- <u>Characterization</u> (processes carried out by Ahn et al. [3])

Using Raman spectroscopy [19], they identified and characterized the graphene monolayer [Figure 9A] [3], which they visualized using high-resolution transmission electron microscopy (HR-TEM) [Figure 9B] [3]. Using field-emission scanning electron microscopy (FE-SEM), they visualized the immobilized nanovesicles on graphene [Figure 9C] [3].
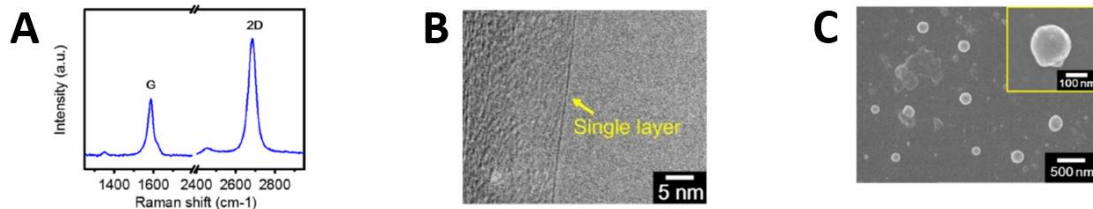

<u>Figure 9</u>. [3] (A) Characteristic Raman spectrum of a graphene monolayer; [3] (B) HR-TEM image of the graphene monolayer; [3] (C) FE-SEM image of the immobilized nanovesicles on graphene.

Regarding the analysis of the electrical properties of the device, they first studied the relation between the source-drain voltage (V_{sd}) and the source-drain current (I_{sd}), before and after the immobilization of nanovesicles on graphene [Figure 10A] [3]. As can be seen, the I_{sd}/V_{sd} relation is linear, experiencing a substantial decrease when the nanovesicles are immobilized on the graphene. This decrease is likely due to the resistance exerted by the nanovesicles to the passage of current between S and D. Once the nanovesicles were immobilized on the graphene, they studied the behavior of the device by measuring the output curves [20], in which I_{sd} is a function of V_{sd} for a fixed gate voltage (V_g) [Figure 10B] [3]. As electrolyte they used DPBS saline solution which contained $CaCl_2$. As can be seen, as the applied gate voltage increases negatively, the I_{sd} also increases negatively. This behavior corresponds to that of a p-type semiconductor [3,21], therefore, the majority charge carriers are the holes.
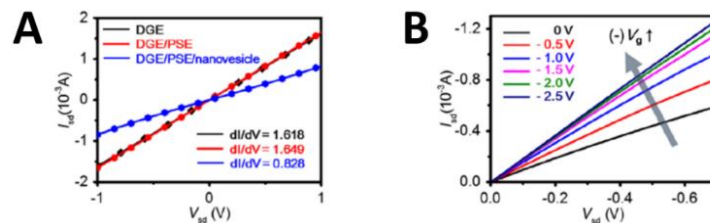

<u>Figure 10</u>. [3] (A) I-V relation before and after the immobilization of the nanovesicles on the graphene; [3] (B) I-V relation given different input voltages across G.

- <u>Results</u> (results obtained by Ahn et al. [3])

The responses obtained by the electronic tongue after the addition of different concentrations of sucrose (sweet ligand), and monosodium glutamate (MSG) (umami ligand), are shown in [Figure 11] [3].
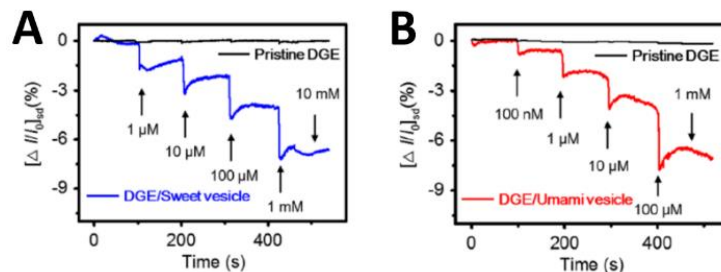

Figure 11. Responses after the addition of different concentrations of [3] (A) sucrose (sweet flavoring) and [3] (B) MSG (umami flavoring).

As can be seen in [Figure 11] [3], increasing the amount of ligand-receptor bindings causes the I_{sd} to decrease. This suggests that the ligand-receptor binding generates a positive gate effect on the graphene, thus reducing the number of holes [3]. Given that the graphene is behaving as a p-type semiconductor, in which the majority charge carriers are the holes, a reduction in the number of holes (through a positive gate effect) leads to the decrease of I_{sd}.

For the sweet taste, the selectivity [Figure 12A] [3] and sensitivity [Figure 12B] [3] of the corresponding sensor were studied using natural sweet ligands (sucrose and fructose), artificial sweet ligands (aspartame and saccharin) and non-sweet ligands (cellobiose and D-glucuronic acid). It stands out in [Figure 12B] [3] that the sensor showed greater sensitivity to artificial sweet ligands than to natural sweet ligands (as occurs in humans). For umami taste, the selectivity [Figure 12C] [3] and sensitivity [Figure 12E] [3] of the corresponding sensor were studied using umami ligands (MSG), non-umami ligands (L-glutamine), umami flavor enhancing ligands (cyclamate and inosine-5'-monophosphate (IMP)) and artificial seasonings (see Ahn et al. [3], *Preparation of Tastants*). As seen in [Figure 12C and 12D] [3], umami flavor-enhancing ligands have an effect on sensor response only in the presence of umami ligands.

Consult (Ahn et al., 2016 [3]) for a more complete analysis of the results obtained for each sensor: minimum detectable level (MDL), signal-to-noise ratio, saturation level, limit of detection (LOD), and response times. The results of the dual response of the electronic tongue to sweet and umami flavors are also shown, which suggest that the studied electronic tongue effectively discriminates target flavors in real food samples [3].
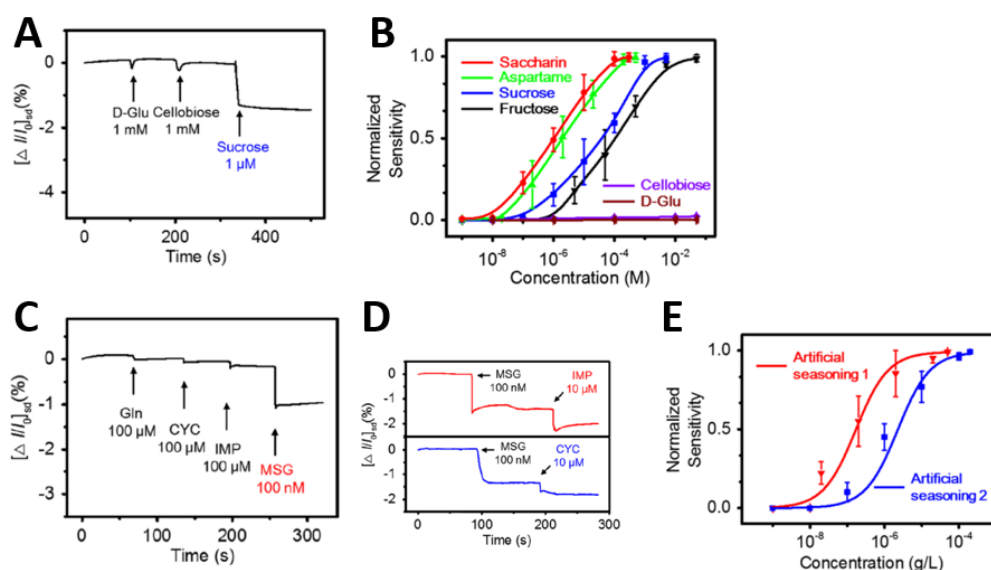
Figure 12. Responses after the addition of different concentrations of [3] (A) cellobiose, D-glucuronic acid, [3] (B) sucrose, fructose, aspartame, saccharin [3] (C, D) L-glutamine, cyclamate, IMP, MSG and [3] (E) artificial seasonings (see Ahn et al.[3], *Preparation of Tastants*).

In summary, the response obtained by the electronic tongue constructed by Ahn et al. [3] for the reception of sweet and umami flavors, resembles the sensory dynamics established in the reception of the same flavors through the sense of taste in humans. The proposed sensors stand out for their high sensitivity and selectivity.

Bibliography

(1)   Marx, Í. M. G.; Veloso, A. C. A.; Casal, S.; Pereira, J. A.; Peres, A. M. Sensory Analysis Using Electronic Tongues. *Innov. Food Anal.* **2021**, 323–343.

(2)   Podrazka, M.; Báczyńska, E.; Kundys, M.; Jeleń, P. S.; Nery, E. W. Electronic Tongue-A Tool for All Tastes? *Biosensors* **2017**, *8* (1), 1–24.

(3)   Ahn, S. R.; An, J. H.; Song, H. S.; Park, J. W.; Lee, S. H.; Kim, J. H.; Jang, J.; Park, T. H. Duplex Bioelectronic Tongue for Sensing Umami and Sweet Tastes Based on Human Taste Receptor Nanovesicles. *ACS Nano* **2016**, *10* (8), 7287–7296.

(4)   Zhang, N.; Wei, X.; Fan, Y.; Zhou, X.; Liu, Y. Recent Advances in Development of Biosensors for Taste-Related Analyses. *TrAC - Trends Anal. Chem.* **2020**, *129*.

(5)   Roper, S. D.; Chaudhari, N. Taste Buds: Cells, Signals and Synapses. *Nat. Rev. Neurosci.* **2017**, *18* (8), 485–497.

(6)   Ahmad, R.; Dalziel, J. E. G Protein-Coupled Receptors in Taste Physiology and Pharmacology. *Front. Pharmacol.* **2020**, *11* (November).

(7)   Miura, R. M. Analysis of Excitable Cell Models. **2002**, *144*, 29–47.

(8)   Vandenbeuch, A.; Kinnamon, S. C. Why Do Taste Cells Generate Action Potentials? **2009**, 2–6.

(9)   Kashio, M.; Wei-qi, G.; Ohsaki, Y.; Kido, M. A.; Taruno, A. CALHM1/CALHM3 Channel Is Intrinsically Sorted to the Basolateral Membrane of Epithelial Cells Including Taste Cells. *Sci. Rep.* **2019**, *9* (1), 1–13.

(10)   Roper, S. D. Taste Buds as Peripheral Chemosensory Processors. *Semin. Cell Dev. Biol.* **2013**, *24* (1), 71–79.

(11)   Larson, E. D.; Vandenbeuch, A.; Voigt, A.; Meyerhof, W.; Kinnamon, S. C.; Finger, T. E. The Role of 5-HT3 Receptors in Signaling from Taste Buds to Nerves. *J. Neurosci.* **2015**, *35* (48), 15984–15995.

(12)   Haick, H. Nanotechnology and Nanosensors. **2013**.

(13)   Moon, D.; Cha, Y. K.; Kim, S. ong; Cho, S.; Ko, H. J.; Park, T. H. FET-Based Nanobiosensors for the Detection of Smell and Taste. *Sci. China Life Sci.* **2020**, *63* (8), 1159–1167.

(14)   Liu, H.; Liu, Y.; Zhu, D. Chemical Doping of Graphene. *J. Mater. Chem.* **2011**, *21* (10), 3335–3345.

(15)   Fechine, G. J. M.; Martin-Fernandez, I.; Yiapanis, G.; Bentini, R.; Kulkarni, E. S.; Bof De Oliveira, R. V.; Hu, X.;

Yarovsky, I.; Castro Neto, A. H.; Özyilmaz, B. Direct Dry Transfer of Chemical Vapor Deposition Graphene to Polymeric Substrates. *Carbon N. Y.* **2015**, *83*, 224–231.

(16)   Venugopal, G.; Kim, S. J. Temperature Dependent Transfer Characteristics of Graphene Field Effect Transistors Fabricated Using Photolithography. *Curr. Appl. Phys.* **2011**, *11* (3 SUPPL.), S381–S384.

(17)   Selvarajan, R. S.; Majlis, B. Y.; Mohamed, M. A.; Hamzah, A. A. Optimization of Lift off Process in Electrode Patterning for Graphene Based Field Effect Transistor. *ASM Sci. J.* **2019**, *12* (SpecialIssue4), 76–82.

(18)   Kim, Y. J.; Lee, Y. G.; Jung, U.; Lee, S.; Lee, S. K.; Lee, B. H. A Facile Process to Achieve Hysteresis-Free and Fully Stabilized Graphene Field-Effect Transistors. *Nanoscale* **2015**, *7* (9), 4013–4019.

(19)   Marquina, J.; Power, C.; González, J. Espectroscopía Raman Del Grafeno Monocapa y El Grafito: Acoplamiento Electrón Fonón y Efectos No Adiabáticos Raman Spectroscopy in Monolayer Graphene and Graphite: *Rev. Tumbaga* **2010**, No. 5, 183–194.

(20)   Béraud, A.; Sauvage, M.; Bazán, C. M.; Tie, M.; Bencherif, A.; Bouilly, D. Graphene Field-Effect Transistors as Bioanalytical Sensors: Design, Operation and Performance. *Analyst* **2021**, *146* (2), 403–428.

(21)   Li, P.; Lei, N.; Xu, J.; Xue, W. High-Yield Fabrication of Graphene Chemiresistors with Dielectrophoresis. *IEEE Trans. Nanotechnol.* **2012**, *11* (4), 751–759.